

Facile and green synthesis of well-dispersed Au nanoparticles in PAN nanofibers by tea polyphenols†

Han Zhu,^b MingLiang Du,^{*ab} MeiLing Zou,^b CongSheng Xu,^b Ni Li^{ab} and YaQin Fu^{ab}

Received 13th December 2011, Accepted 7th March 2012

DOI: 10.1039/c2jm16569d

The green natural compounds, tea polyphenols (TP), were introduced to synthesize well-dispersed Au nanoparticles (AuNPs) in polyacrylonitrile (PAN) nanofibers by combining an *in situ* reduction approach and electrospinning technique. The AuNPs were firstly synthesized in aqueous solution to test the reducibility of the TP. Then, the well-dispersed AuNPs in PAN nanofibers were obtained by an *in situ* reduction approach and electrospinning technique. Fourier transform infrared spectroscopy (FTIR) was utilized to confirm the reducibility of TP. The transmission electron microscopy (TEM) and the ultraviolet-visible spectroscopy (UV-Vis) demonstrated the formation of AuNPs and their morphology. Surprisingly, compared with the AuNPs in aqueous solution, the AuNPs in PAN nanofibers *via* electrospinning were much smaller and well-dispersed and it was attributed to the stabilization effect of PAN through the chelating effect between gold and cyano groups. Apart from the reducibility effect, TP also served as a stabilizer together with PAN to prevent the aggregation of AuNPs effectively, which were testified by X-ray photoelectron spectroscopy (XPS) results.

Introduction

Nanostructured noble metals are widely used in various technological applications due to their unique optical, electronic, imaging, magnetic and catalytic properties.^{1–5} Haruta *et al.* have found that the Au nanoparticles as small as 2 nm showed an excellent catalytic property for total oxidation of CO.⁶ Meanwhile, gold-based nanotechnology is becoming more and more significant in modern science and various kinds of applications of Au nanoparticles (AuNPs) have been explored both in chemical and biological research.^{7,8} Highly dispersed AuNPs have been discovered to be exceptionally active for a number of chemical reactions, such as oxidation and reduction.⁹ A particular attraction is the use of functional AuNPs in pharmaceutical and biological fields, such as drug delivery, photothermal ablation therapy and molecular diagnostics, because AuNPs have excellent biological biocompatibility and low toxicity.^{10–15}

There are already many methods for the synthesis of AuNPs, however, most are either complex, time-consuming, or require strict synthetic conditions.^{12–20} From the viewpoint of practical applications, it would be of great value to explore a facile approach for the synthesis of uniform AuNPs with small particle

sizes. The previous widely adopted methods of synthesizing AuNPs often involve a chemical reductant, such as sodium borohydride and hydrazine, *etc.* These reducing agents are highly active and have potential environmental risks, which might be an issue for wide application. In the present investigation, we proposed a facile and environmental friendly approach to synthesize AuNPs with a small size and narrow distribution using tea polyphenols (TP) as the reductant.¹⁵ TP compounds, which are a group of water-soluble polyphenols richly deposited in plants, belonging to the flavonoid family, mainly consist of epicatechin (EC), epicatechin gallate (ECG), epigallocatechin (EGC) and epigallocatechin gallate (EGCG), in which the EGCG makes up about 45% of the total TP.^{21–23} Studies have shown that such compounds possess many properties, such as reducibility, chelating with metal ions, antibacterial activity, *etc.*^{24–27} However, until now, no reports are found on the synthesis of gold nanoparticles using TP.

Electrospinning technique is an effective method to obtain fibers with nanoscale diameter and nanofibers that are prepared in the form of a non-woven mat possess high specific surface area and high porosity and, subsequently, are ideal substances for tissue engineering scaffolds, catalytic carriers and filter materials.^{28–31,34} Xia *et al.* have studied electrospun TiO₂ nanofibers with Pt nanoparticles and nanowires for catalytic applications, showing us a great prospect for catalysis.³² It is well-recognized that AuNPs exhibit high catalytic activities for certain chemical reactions, moreover, the particle size of AuNPs is often essential to the catalytic activities. Shao's group showed that AuNPs of 3–5 nm in silica nanotubes exhibited a good catalytic activity for reducing 4-nitrophenol.³⁴ Shi's group synthesized collagen

^aKey Laboratory of Advanced Textile Materials and Manufacturing Technology, Zhejiang Sci-Tech University, Ministry of Education, Hangzhou 310018, P. R. China. E-mail: du@zstu.edu.cn; Tel: +86-571-86843255

^bDepartment of Materials Engineering, College of Materials and Textile, Zhejiang Sci-Tech University, Hangzhou 310018, P. R. China

† Electronic supplementary information (ESI) available. See DOI: 10.1039/c2jm16569d

fiber-supported AuNPs with an effective size control in the range 5–18 nm and found that the catalytic behaviors depended on the nanoparticle size and the AuNPs of 5.2 ± 1.6 nm showed the best activity for the reduction of 4-nitrophenol.⁹

In this paper, we reported a facile and green route to synthesize AuNPs/PAN nanofibers *via* an *in situ* reduction approach by TP and electrospinning technique. At first, we confirmed the availability of synthesizing AuNPs using TP as the reductant in aqueous solution. Then, we combined the electrospinning method and the green reducibility of the TP to fabricate AuNPs/PAN nanofibers containing well-dispersed AuNPs. The availability of the reducing method and the fabrication approach were tested, meanwhile, the morphology and structure of the synthesized AuNPs were characterized and discussed.

Experimental

Materials

Chloroauric acid ($\text{HAuCl}_4 \cdot 4\text{H}_2\text{O}$, 99.9%) was acquired from Shanghai Civi Chemical Technology Co., Ltd. Polyacrylonitrile (PAN, $M_w \approx 1.4 \times 10^5$, copolymerized with 10 wt% methyl acrylate) was manufactured by Sinopec Shanghai Petrochemical Co., Ltd. Tea polyphenols (TP) were purchased from Xuancheng BaiCao Plant Industry and Trade Co., Ltd. and the main ingredients are tabulated in Table 1. Dimethyl formamide (DMF, 99.5%) was obtained from Hangzhou Gaojing Fine Chemical Co., Ltd.

Synthesis of AuNPs in aqueous solution using TP as reductant

The AuNPs were synthesized using TP as the reducing agent. 1 mmol $\text{HAuCl}_4 \cdot 4\text{H}_2\text{O}$ was dissolved in 100 mL deionized water to get a 10.0 mmol L^{-1} Au(III) solution. Then, 3 mL Au(III) solution (0.03 mmol Au(III)) was added to 40 mL deionized water. The mixture was heated to 65°C and vigorously stirred by magnetic force and then 0.012 g TP dissolved in 7 mL deionized water was added to the mixture. Samples were taken at different reaction times and then refrigerated at 4°C . The reaction times of each sample were 1 min, 15 min, 30 min, 60 min and 120 min.

Synthesis of AuNPs in PAN/DMF solution with TP

0.067 mmol PAN powder was dissolved in 60 mL DMF under magnetic stirring at 65°C and 0.6 mmol $\text{HAuCl}_4 \cdot 4\text{H}_2\text{O}$ dissolved in 30 mL DMF were dropped into the PAN/DMF

solution. 0.025 g TP were dissolved in 10 mL DMF at room temperature and then immediately added drop-wise to the above PAN/DMF solution. Therefore, the mass fraction of PAN in the DMF solution was 10 wt% and the mass ratio of $\text{HAuCl}_4 \cdot 4\text{H}_2\text{O}$ and the PAN powder was 2.5 wt%. The mixture was stirred by magnetic agitator for 300 min. Samples were taken at different reaction times and the samples were refrigerated at 4°C . The reaction times of each sample were 30 min, 60 min, 120 min, 200 min, 300 min and 400 min.

Electrospinning of AuNPs/PAN nanofibers

The above mixture solution with a reaction time of 60 min and mass ratio of 2.5 wt% ($\text{HAuCl}_4 \cdot 4\text{H}_2\text{O}$ to PAN) was used to prepare a non-woven mat *via* electrospinning technique. The solution was transferred into a syringe with a stainless copper needle at the tip. The needle was connected to a high voltage power supply. The applied voltage was 12 kV, the needle to collector distance was 12 cm and the flow rate of the solution was 0.01 mL min^{-1} . All experiments were performed at room temperature. The electrospun nanofibers were collected onto a piece of aluminum foil. Finally, the nanofiber mats were peeled off from the aluminum foil and kept in polyethylene sealing bags.

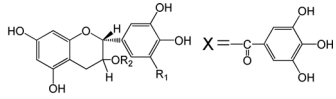
Characterization

Fourier transform infrared spectroscopy (FTIR). A thin layer of the prepared solutions obtained from various aged reaction times was spread on KBr pellets individually and then dried at room temperature. The FTIR analysis was conducted by an Image-Pro Nicolet 5700 FTIR spectrometer.

Ultraviolet-visible spectroscopy (UV-Vis). The as-prepared AuNPs in the aqueous solution and the AuNPs in PAN/DMF solution were examined by a Lambda 900 UV-Vis spectrophotometer (Perkin Elmer, USA), and the reference solutions were treated with deionized water and DMF, respectively. To confirm the reducibility of TP for Au(III) ions, the UV-Vis spectra of TP heated for different times at 65°C were also tested. All the spectra were collected over a wavelength range of 200–800 nm.

Transmission electron microscopy (TEM) and high resolution transmission electron microscopy (HRTEM). The diluted AuNPs in aqueous solution were dropped on the ultra-thin carbon-coated copper grid and dried under an infrared lamp for 5 min.

Table 1 The main ingredients of TP

Ingredients	Percentage	Structural Formula
Epigallocatechin (EGC)	12.3%	 <p> $R_1=\text{OH}, R_2=\text{H}$, EGC $R_1=\text{OH}, R_2=\text{X}$, EGCG $R_1=R_2=\text{H}$, EC $R_1=\text{H}, R_2=\text{X}$, ECG </p>
Catechin gallate (EGCG)	45.3%	
Catechin (EC)	4.3%	
Epicatechin gallate (ECG)	9.1%	

The electrospun nanofibers were placed on the ultra-thin carbon-coated copper grid and dried under an infrared lamp for 5 min. The images were acquired using JSM-2100 transmission electron microscopy (TEM, JEOL, Japan) at an accelerating voltage of 200 kV. The sizes of AuNPs (200 counts) were measured with Image-Pro Plus 6.2 software.

Field emission scanning electron microscopy (FE-SEM). The nanofiber mats were plated with a thin layer of gold before observations. The morphology of the electrospun AuNPs/PAN nanofibers was observed by a JSM-6700F field-emission scanning electron microscope (FE-SEM, JEOL, Japan). The diameters of AuNPs/PAN nanofibers (100 counts) were measured with Image-Pro Plus 6.2 software.

X-ray photoelectron spectroscopy (XPS). X-ray photoelectron spectra of pure PAN powder, TP and AuNPs/PAN nanofibers were recorded using an X-ray Photoelectron Spectrometer (Kratos Axis Ultra DLD) with an aluminum (mono) K_{α} source (1486.6 eV). The aluminum K_{α} source was operated at 15 kV and 10 mA. For all of the samples, a low-resolution survey run (0–1100 eV, pass energy = 160 eV) was performed. In order to obtain more information about the chelating effect, a high-resolution survey (pass energy = 48 eV) was performed at spectral regions relating to gold, oxygen and nitrogen.

Results and discussion

Synthesis of well-separated AuNPs in the aqueous reduced by TP

The TEM images of AuNPs in the aqueous solution are shown in Fig. 1. Fig. 1A, with the corresponding insets, portrays the morphology of the AuNPs with a reducing time of 60 min. The average diameter of AuNPs shown in Fig. 1C was about 23.8 ± 6.1 nm. As mentioned above, TP was a mixture of different polyphenols, therefore the synthesized AuNPs exhibited a relatively wide size distribution. The insets located in the lower right corner of Fig. 1A and D indicate that the AuNPs were spherical and well-separated in aqueous solution. Fig. 1D showed that the

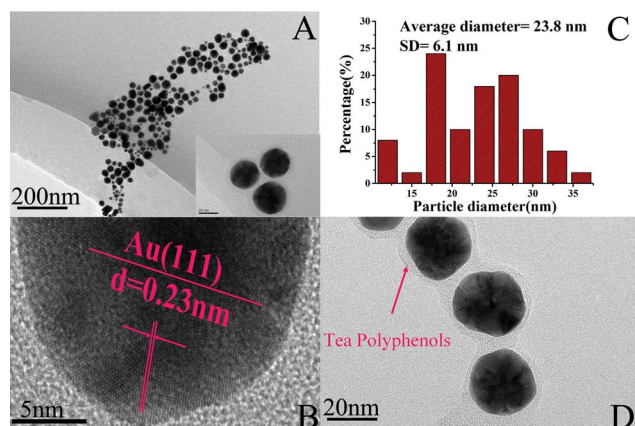


Fig. 1 (A, D) TEM images of the morphology of the AuNPs and (C) the corresponding particle size distribution of AuNPs. (B) The HRTEM image of AuNPs. The inset in (A) shows the well-separated AuNPs. The reduction time of the sample is 60 min.

AuNPs were coated with a layer of TP (with thickness of 2–3 nm, as shown in Fig. S1, see ESI†) and separated well, suggesting a stabilization effect of TP for AuNPs, which will be discussed later. The lattice fringes shown in Fig. 1B were visible with a spacing of about 0.23 nm, which corresponded to the lattice spacing of the (111) planes of Au.

Fig. 2 shows the UV-Vis absorption spectra taken at different intervals after mixing HAuCl_4 aqueous solution with TP aqueous solution. The mixture solutions were transparent and the color changed from golden yellow to deep purple with the increasing reaction time. In Fig. 2, the TP solution (curve a) and TP solution heated for 120 min at 65°C (curve h) both showed an absorption peak around 275 nm. In addition, as shown in Fig. 2S (see ESI†), all of the samples heated at 65°C for different times also showed the same absorption peak around 275 nm. There's no evolution for the UV-Vis spectra curves of the TP and all of the heated samples, indicating that the heating (65°C) was not sufficient to oxidize TP. An absorption peak at 290 nm appeared in curve b and is a result of the charge transfer between the gold and chloro ligands.^{14,37} When TP was added to the chloroauric acid solution, the absorption peak at 290 nm vanished because of the reduction of Au(III) by TP. In addition, a new peak emerged at 580 nm and the absorption peak of AuNPs can be considered as a superposition of the contribution from intraband transitions, which is believed to be a consequence of photoexcitation of the free conduction electrons on the surface of AuNPs.^{33,36} According to the literature,^{14,33} a strong and sharp peak around 275 nm also corresponds to Au clusters or small NPs due to the inter-band transitions, which may be overlaid with the absorption of TP in the present investigations. The broad band around 580 nm was assigned to the surface plasma resonance of larger Au nanoparticles.

The broad band indicated a relatively high polydispersity of the AuNPs, both in size and shape. Very interestingly, a comparison of the spectra showed that with a reaction time increase from 1 min to 120 min, the surface plasmon resonance band had a hypsochromic shift from 580 nm to 560 nm. It is

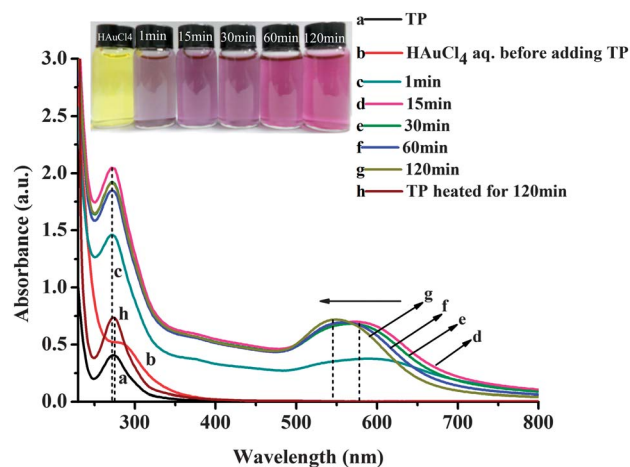
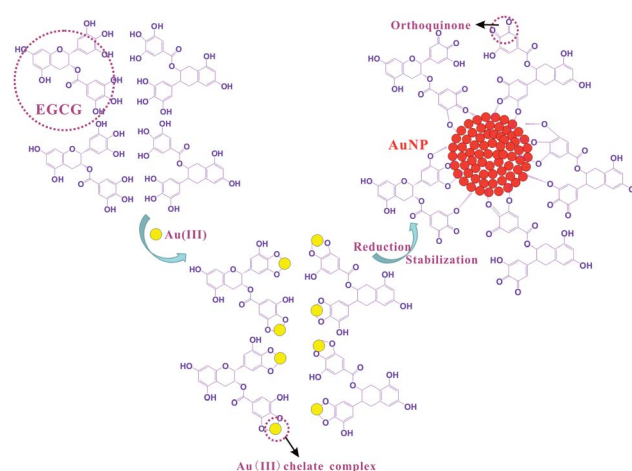


Fig. 2 UV-Vis absorption spectra of (a) TP, (h) TP heated for 120 min, (b) HAuCl_4 aq. before adding TP and (c–g) AuNPs in aqueous solution at different reaction times. The insets are the color of the corresponding samples at different reaction times.

well-established that such hypsochromic shifts in the UV-Vis spectrum are related to chemical changes in the environment.^{33,36} Thus, the observed shifts here would be in accordance with the reduction of Au ions through TP, followed by structural changes in the TP molecules. All of the above information confirmed the reducing and protective actions of the green compounds and it shows a great perspective for reducing other noble metal without introducing any hazardous substances.

Further research was done to test the reducibility of TP for synthesizing AuNPs. The FTIR spectra of TP and the oxidized TP and the chemical changes before and after oxidation are indicated in Fig. 3. The absorption peaks at 1455 cm⁻¹ and 1096 cm⁻¹ assigned to C–H alkanes in aromatic rings and C–O–C stretching vibration did not change during the reaction process. Based on the comparison spectrum of oxidized TP, the emerging absorption band at 2367 cm⁻¹ in oxidized TP was ascribed to the stretching vibration of C=O, suggesting the formation of the orthoquinone structure in TP. The obvious weak absorption peaks at 1344 cm⁻¹ and 1037 cm⁻¹ belong to the O–H in-plane bending vibration and C–O–H stretching vibration of phenolic hydroxyls in TP, respectively, which were results of the oxidation. The absorption band around 3371 cm⁻¹ shifted to 3414 cm⁻¹ and became relatively narrow, which also implied the involvement of the O–H groups in the reduction of Au ions, resulting in the partial destruction of hydrogen bonds among TP molecules. In addition, the damping absorption peak at 1147 cm⁻¹ assigned to O–H aromatic further indicated that the reduction of Au ions could be coupled to orthoquinone groups of oxidized TP.^{9,14,25,35} All of the above data further confirmed the reducibility of TP and indicated that the phenolic hydroxyls were oxidized to orthoquinone.

The reaction mechanism for the formation of AuNPs in aqueous solution by TP reduction is illustrated in Scheme 1. As a typical plant polyphenol, TP was a mixture of different polyphenols with multiple orthophenolic hydroxyls, which could have various reducing capabilities. As the main ingredients of TP, EGCG was employed for the mechanisms instead of TP. As reported in the literature, EGCG has been proven to be an



Scheme 1 A schematic illustration of the mechanism for the formation and stabilization of AuNPs in aqueous solution reduced by EGCG (the main ingredients of TP).

excellent bidentate ligand to bond with Au(III) ions by forming a stable five-member chelating ring.^{9,14} The orthophenolic hydroxyls can chelate with the Au(III) ions, leading to the formation of a Au(III) chelate complex. Then, the chelated Au(III) ions were reduced into Au⁰ atoms *in situ*, while a part of the phenolic hydroxyls of EGCG are simultaneously oxidized to the corresponding carbonyl groups, orthoquinone.^{9,14} According to Tripathy's research,²⁶ both the formed carbonyls and free hydroxyls are able to stabilize AuNPs by the interaction between the surface Au atoms of AuNPs and oxygen atoms of EGCG molecules.

Preparation of AuNPs/PAN nanofibers by electrospinning technique

In the above work, we confirmed the availability of the reducibility of TP in synthesizing AuNPs in aqueous solution and obtained well-separated AuNPs with an average diameter of about 23.8 ± 6.1 nm successfully. In the following work, we described an effective facile route to fabricate AuNPs/PAN nanofibers with a well-dispersed distribution of small AuNPs, which would be used potentially for catalytic applications. It was obviously seen in Fig. 4A and C that the AuNPs were spherical and well-dispersed in the PAN nanofibers. The average diameter of the AuNPs embedded in PAN nanofibers was 4.8 ± 1.1 nm. The morphology of the AuNPs in PAN/DMF precursor solution before electrospinning was shown in Figs 3S and 4S (see ESI†). In Fig. 4D, the latter fringe spacing of AuNPs was about 0.23 nm, which corresponded to the (111) plane.⁴² Compared with the AuNPs in the aqueous solution, the diameter of AuNPs embedded in PAN nanofibers was one order of magnitude smaller than these in aqueous solution and had a narrow distribution of diameter. Therefore, it is concluded that the PAN polymer might play a crucial role of stabilizer and direct the particular arrangements of Au nanoparticles during the reduction and electrospinning process.

The UV-Vis absorption spectra of the AuNPs/PAN nanofiber precursor solution with different reaction times are shown in Fig. 5. With an increase of reaction time, the solution colors

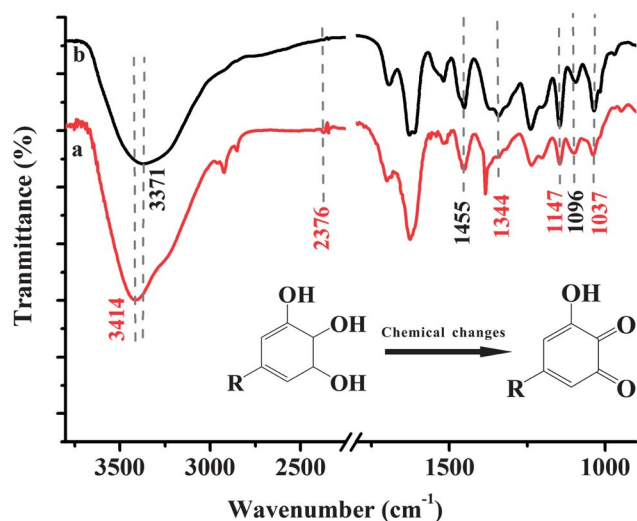


Fig. 3 The FTIR spectra of (a) TP and (b) TP after oxidation.

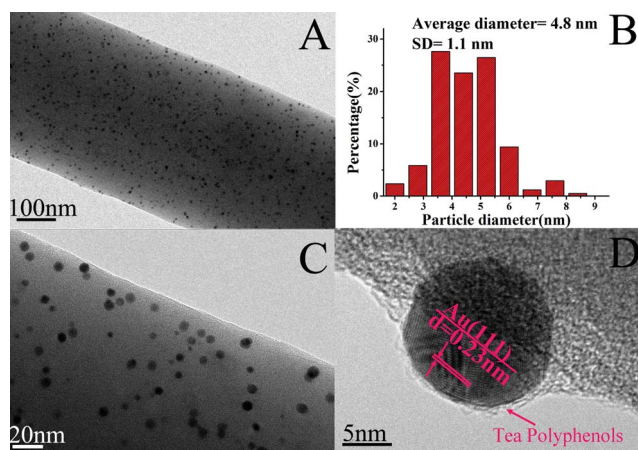


Fig. 4 (A, C) TEM images of the AuNPs/PAN nanofibers, (B) the corresponding particle size distribution of the AuNPs. (D) The HRTEM image of the AuNP embedded in PAN nanofibers.

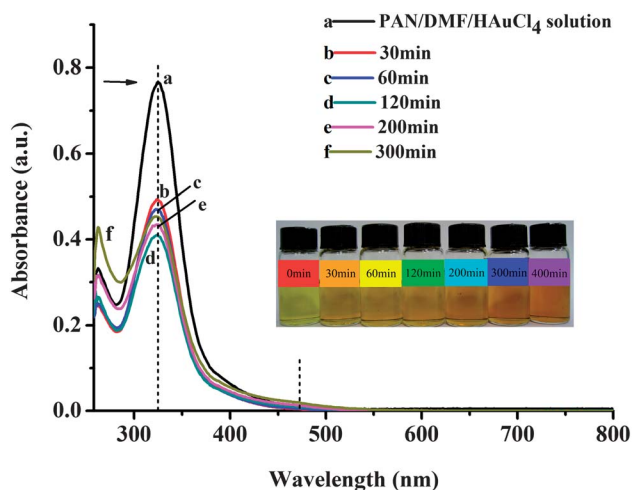
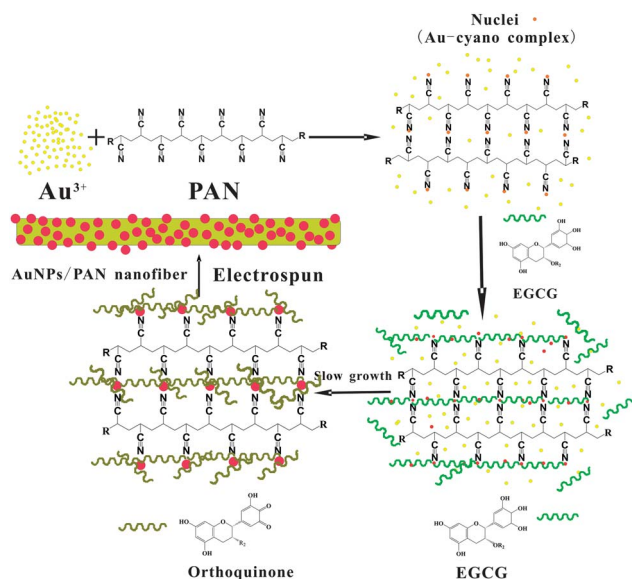


Fig. 5 Temporal evolution of UV-Vis absorption spectra after addition of TP into HAuCl₄/PAN/DMF solution. The insets show the corresponding samples at different reaction times.

changed from gold-yellow to orange-red. However, there was no dramatic UV peak shift. The two narrow UV peaks remained at around 261 nm and 323 nm. The absorption peak around 261 nm was assigned to the characteristic peak of the AuNPs in the nanofibers precursor solution. With the increase of the reducing time from 30 min to 300 min, the peak around 261 nm exhibited a red-shift from 261 nm to 263 nm (from curve b to curve f) and becomes more intense, which is attributed to the decrease of the particle size.^{18,33} Another absorption peak at 323 nm was assigned as the characteristic for PAN.^{30,45,46} Comparing with the UV-Vis absorption spectra in Fig. 5 and Fig. 2, we found that the absorption around 580 nm hypsochromic shifts to about 470 nm and became relatively weak, suggesting the nearly disappearance of larger size of AuNPs, which was in accordance with the results of TEM images in Fig. 4 and Fig. 1.

The present process of fabrication of the AuNPs/PAN nanofibers is schematically illustrated in Scheme 2. It has been known that the main chains of PAN polymer possess a large number of



Scheme 2 A schematic illustration of the mechanism for the fabrication of AuNPs/PAN nanofibers.

cyano groups that have one lone electron pair and can form a chelate complex with the Au ions.^{9,38,44} The functional groups can effectively catch the Au ions, leading to the formation of Au-cyano complexes through the chelating effect.^{9,30} The synthesis of AuNPs of different sizes was a kinetically driven process.^{38,39}

At the beginning of the process, the PAN polymer firstly seized the Au ions through chelating effect, and then formed a Au-cyano nucleus. Due to the chelating effect between the Au ion and cyano in PAN, the nuclei cannot collide with each other to aggregate easily. In addition, because of the high viscosity of the solution, the diffusion of the Au ions was slow and resulted in the nucleus growing at a relatively low rate. When the TP solution is added to the precursor solution, the Au ions can also chelate with the phenolic hydroxyls of TP. Thus the Au ions were further diffused to the Au nucleus region and reduced on the surface of Au nuclei by TP with the oxidation of the phenolic hydroxyls to orthoquinone. As a consequence, the synthesized AuNPs were wrapped with a layer of TP (with a thickness of 0.5–1 nm, as shown in Fig. S1 in ESI†), which can be seen in Figs 1D and 4D. FTIR spectra of the AuNPs synthesized with TP in the presence of PAN and embedded in the PAN nanofibers are shown in Figs 5S and 6S (see ESI†). These FTIR spectra also confirmed that the AuNPs reduced by TP were coupled with orthoquinone groups of oxidized TP. The cooperation between the chelating effect of cyano in PAN and the phenolic hydroxyls of TP with gold meant that the size and morphology of the as-synthesized AuNPs were small, well-dispersed and possessed a narrow diameter distribution, as demonstrated in Fig. 4.

In a word, the PAN polymer acted as a chelating agent and the TP served as both a reductant and stabilizer during our facile and green approach to synthesize the well-dispersed small AuNPs.

The chelating effects of Au ions with cyano groups in PAN molecules and hydroxyl groups in TP molecules were tested by XPS. Fig. 6A showed the XPS spectrum in the Au 4f region of the AuNPs/PAN nanofibers. It can be seen from the spectrum that the two XPS peaks at 88.0 eV and 84.5 eV were in agreement

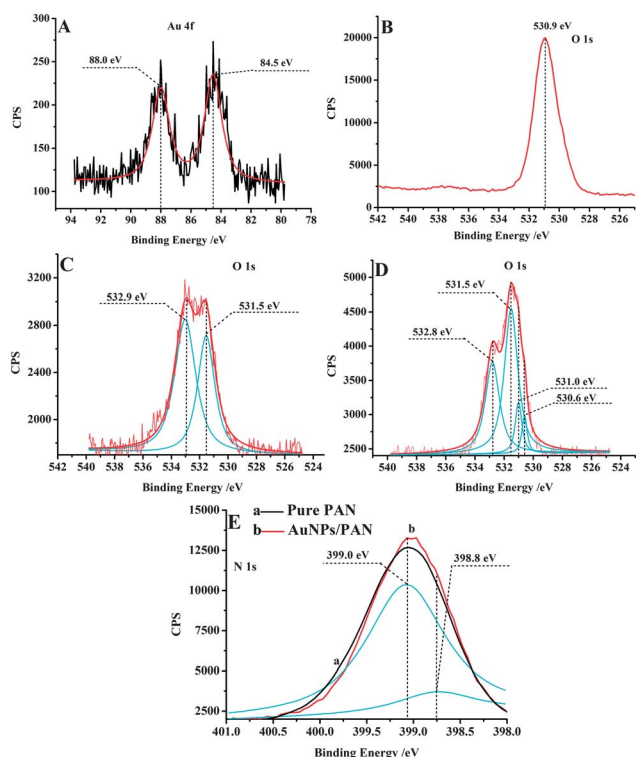


Fig. 6 XPS spectra of the electrospun nanofibers, pure PAN and TP: (A) Au 4f of PAN/AuNPs nanofibers; (B) O 1s of TP; (C) O 1s of the pure PAN; (D) O 1s of PAN/AuNPs nanofibers; (E) N 1s of the comparison between pure PAN powder and AuNPs/PAN nanofibers.

with the binding energies of Au 4f_{7/2} and Au 4f_{5/2}, respectively. Compared with Au⁰ (87.7 eV and 84.0 eV),^{9,26} the changes in the binding energy indicated the chelating effects between Au ions and PAN molecules. The oxygen 1s XPS spectra of TP, pure PAN and AuNPs/PAN nanofibers are shown in Fig. 6B, C and D. TP showed a single O 1s XPS peak at 530.9 eV, while pure PAN had two O 1s peaks at 531.5 eV and 532.9 eV, which was due to the two different chemical environments of oxygen in methyl acrylate (PAN contains 10 wt% of methyl acrylate). As for the O 1s XPS spectra of AuNPs/PAN nanofibers in Fig. 6D, after the peak separation with Origin 8.0 software, there were mainly three peaks at 530.9 eV, 531.5 eV and 532.8 eV, which were thought to be from TP and methyl acrylate in PAN, respectively. It is believed that the new emerging peak at 531.0 eV was a result of the strong coordination between AuNPs and oxygen.^{9,39,43} From Figs 1D and 4D, it can be seen that the AuNPs were encapsulated with a layer of TP molecules, which could restrain the AuNPs from aggregation during the synthesis process. In addition, there was a binding energy shift of oxygen 1s from 530.9 eV to 530.6 eV in TP before and after reduction, while there was nearly no shift for the oxygen 1s in methyl acrylate. Tanaka and Negishi have found that the relatively high binding energy of Au 4f was due to the binding of surface Au atoms in AuNPs with the stabilizer or passive molecules surrounding the nanoparticles, which led to a substantial electron donation from AuNPs to the stabilizer molecules.^{40,41}

The XPS spectra of the nitrogen 1s in pure PAN and AuNPs/PAN nanofibers are shown in Fig. 6E. The strong peak at 399.1 eV exists both in pure PAN (curve a) and AuNPs/PAN

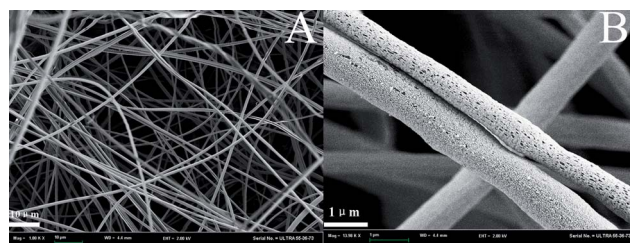


Fig. 7 (A) FE-SEM image of a non-woven mat of AuNPs/PAN nanofibers. (B) A highly magnified FE-SEM image of the AuNPs/nanofibers.

nanofibers (curve b), suggesting nearly no change of the chemical environment for most of the nitrogen in PAN molecular chains. However, a relatively weak peak of nitrogen 1s was occurred at 398.8 eV and it is concluded that the C≡N groups on the surface of PAN nanofibers may be involved in the interaction with AuNPs.⁴⁴ In other words, there was coordination between AuNPs and nitrogen, which was helpful for the synthesis of AuNPs with a smaller size and good distribution. Based on the above effects, the AuNPs with a diameter around 5 nm were formed and well-dispersed in PAN nanofibers. On the basis of all of the above data, we confirmed that the green TP can serve both as a reductant and stabilizer during the reaction process, and the PAN polymer can also be used as a stabilizing agent to prevent aggregation due to the chelating effect between the cyano groups and Au ions.

Fig. 7 shows the FE-SEM images of the non-woven mat of AuNPs/PAN nanofibers *via* electrospinning technique. As illustrated in Fig. 7A, there is a three-dimensional network structure consisting of a large quantity of randomly deposited nanofibers and the average diameter of AuNPs/PAN nanofibers was about 780 ± 170 nm, which is shown in Fig. 8S (see ESI†). More FE-SEM images are shown in Fig. 7S (see ESI†). Fig. 7B indicates that the surface of the nanofibers was relatively rough and porous, which can provide a high specific surface area. As previously discussed, the AuNPs were synthesized and well-dispersed in the PAN nanofibers, which was promising for the potential catalytic application. Due to the rough and porous surface of the nanofibers, we will explore the synthesis of noble nanoparticles on the surface and in the pores of the nanofibers, which would possess more catalytic activity.

Conclusion

In this study, we showed a green and facile synthesis of well-dispersed small AuNPs embedded in the electrospun PAN nanofibers by combining an electrospinning technique and *in situ* reduction approach. The UV-Vis spectra of the AuNPs synthesized in the aqueous and PAN/DMF solutions confirmed the reduction of TP and the formation of AuNPs. The morphology of the formed AuNPs were characterized by TEM. In our synthetic route, the PAN worked as a stabilizer to catch the Au ions through the chelating effect and formed an Au-cyano nucleus and then the Au ions were reduced by TP. The results of FTIR and XPS confirmed the reducibility of TP and indicated the interaction between the AuNPs with TP and PAN. The FE-SEM indicated that the as-prepared AuNPs/PAN nanofibers exhibited a relatively rough and porous surface, which might

provide a bright prospect for the catalytic activity. This new route provides a useful approach for the fabrication of nano-catalysts based on a noble metal.

Acknowledgements

This work is supported by the project of National Natural Science Foundation of China (NSFC) (Grant number: 50903072, 10902099), Zhejiang Province Natural Science Foundation (Grant number: Y4100197) and Science Foundation of Zhejiang Sci-Tech University (ZSTU) under No. 0901803-Y.

References

- 1 H. Tsunoyama, H. Sakurai, N. Ichikuni, Y. Negishi and T. Tsukuda, *Langmuir*, 2004, **20**, 11293–11296.
- 2 P. Migowski and J. Dupont, *Chem.–Eur. J.*, 2007, **13**, 33–39.
- 3 R. C. Jin, Y. W. Cao, C. A. Mirkin, K. L. Kelly, G. C. Schatz and J. G. Zheng, *Science*, 2001, **294**, 1901–1903.
- 4 A. S. K. Hashmi and G. J. Hutchings, *Angew. Chem.*, 2006, **118**, 8064–8105.
- 5 X. Fang, H. Ma, S. L. Xiao, M. W. Shen, R. Guo, X. Y. Cao and X. Y. Shi, *J. Mater. Chem.*, 2011, **21**, 4493–4501.
- 6 M. Haruta, M. Yamata, T. Kobayashi and S. Lijima, *J. Catal.*, 1989, **115**, 301–309.
- 7 A. Rai, A. Prabhune and C. C. Perry, *J. Mater. Chem.*, 2010, **20**, 6789–6798.
- 8 Y. W. Cao, R. Jin and C. A. Mirkin, *J. Am. Chem. Soc.*, 2001, **123**, 7961–7962.
- 9 H. Wu, X. Huang, M. M. Gao, X. P. Liao and B. Shi, *Green Chem.*, 2011, **13**, 651–658.
- 10 J. J. Zhang, M. M. Gu, T. T. Zheng and J. J. Zhu, *Anal. Chem.*, 2009, **81**, 6641–6648.
- 11 S. Liu, G. Y. Chen, P. N. Prasad and M. T. Swihart, *Chem. Mater.*, 2011, **23**, 4098–4101.
- 12 E. Thimsen, *Chem. Mater.*, 2011, **23**, 4612–4617.
- 13 Z. C. Xu, Y. L. Hou and S. H. Sun, *J. Am. Chem. Soc.*, 2007, **129**, 8698–8699.
- 14 X. Huang, H. Wu, X. P. Liao and B. Shi, *Green Chem.*, 2010, **12**, 395–399.
- 15 M. C. Moulton, L. K. Braydich-Stolle, M. N. Nadagouda, S. Kunzelman, S. M. Hussain and R. S. Varma, *Nanoscale*, 2010, **2**, 763–770.
- 16 M. Schulz-Dobrick, K. V. Sarathy and M. Jansen, *J. Am. Chem. Soc.*, 2005, **127**, 12816–12817.
- 17 A. Rai, A. Prabhune and C. C. Perry, *J. Mater. Chem.*, 2010, **20**, 6789–6798.
- 18 J. Garcia-Serrano, U. Pal, A. M. Herrera, P. Salas and C. Angeles-Chavez, *Chem. Mater.*, 2008, **20**, 5146–5153.
- 19 C. Kruger, S. Agarwal and A. Greiner, *J. Am. Chem. Soc.*, 2008, **130**, 2710–2711.
- 20 A. N. Shipway, M. Lahav and I. Willner, *Adv. Mater.*, 2000, **12**, 993–997.
- 21 S. Tsubaki, H. Iida, M. Sakamoto and J. Azuma, *J. Agric. Food Chem.*, 2008, **56**, 11293–11299.
- 22 Y. Wang, Z. X. Shi and J. Yin, *ACS Appl. Mater. Interfaces*, 2011, **3**, 1127–1133.
- 23 Y. N. Chen, Y. D. Lee, H. Vedala, B. L. Allen and A. Star, *ACS Nano*, 2010, **4**, 6854–6862.
- 24 A. Yella, H. W. Lee, H. N. Tsao, C. Y. Yi, A. K. Chandiran, M. K. Nazeeruddin, E. W. G. Diau, C. Y. Yeh, S. M. Zakeeruddin and M. Grätzel, *Science*, 2011, **334**, 629–633.
- 25 Y. S. Park, M. K. Lee, B. G. Heo, K. S. Ham, S. G. Kang, J. Y. Cho and S. Gorinstein, *Plant Foods Hum. Nutr.*, 2010, **65**, 186–191.
- 26 P. Tripathy, A. Mishra, S. Ram, H.-J. Fecht, J. Bansmann and R. J. Behm, *Nanotechnology*, 2009, **20**, 075701.
- 27 L. L. Song, R. Liang, D. D. Li, Y. D. Xing, R. M. Han, J. P. Zhang and L. H. Skibsted, *J. Agric. Food Chem.*, 2011, **59**(23), 12643–12651.
- 28 D. He, B. Hu, Q. F. Yao, K. Wang and S. H. Yu, *ACS Nano*, 2009, **3**, 3993–4002.
- 29 G. M. Kim, A. Wutzler, H. J. Radusch, G. H. Michler, P. Simon, R. A. Sperling and W. J. Parak, *Chem. Mater.*, 2005, **17**, 4949–4957.
- 30 J. Bai, Y. X. Li, M. Y. Li, S. G. Wang, C. Q. Zhang and Q. B. Yang, *Appl. Surf. Sci.*, 2008, **254**, 4520–4523.
- 31 X. H. Li, C. L. Shao and Y. C. Liu, *Langmuir*, 2007, **23**, 10920–10923.
- 32 E. Formo, E. Lee, D. Campbell and Y. N. Xia, *Nano Lett.*, 2008, **8**, 668–672.
- 33 S. Pocovi-Martínez, M. Parreno-Romero, S. Agouram and J. Perez-Prieto, *Langmuir*, 2011, **27**, 5234–5241.
- 34 Z. Y. Zhang, C. L. Shao, P. Zou, P. Zhang, M. Y. Zhang, J. B. Mu, Z. C. Guo, X. H. Li, C. H. Wang and Y. C. Liu, *Chem. Commun.*, 2011, **47**, 3906–3908.
- 35 R. J. Liao, Z. H. Tang, Y. D. Lei and B. C. Guo, *J. Phys. Chem. C*, 2011, **115**, 20740–20746.
- 36 J. Guan, L. Jiang, J. Li and W. S. Yang, *J. Phys. Chem. C*, 2008, **112**, 3267–3271.
- 37 P. D. Cozzoli, M. L. Curri, C. Giannini and Angela Agostiano, *Small*, 2006, **2**, 413–421.
- 38 C. Q. Zhang, Q. B. Yang, N. Q. Zhan, L. Sun, H. G. Wang, Y. Song and Y. X. Li, *Colloids Surf., A*, 2010, **362**, 58–64.
- 39 S. G. Gholap, M. V. Badiger and C. S. Gopinath, *J. Phys. Chem. B*, 2005, **109**, 13941–13947.
- 40 Y. Negishi, K. Nobusada and T. Tsukuda, *J. Am. Chem. Soc.*, 2005, **127**, 5261–5270.
- 41 A. Tanaka, Y. Takeda, M. Imamura and S. Sato, *Phys. Rev. B: Condens. Matter*, 2003, **68**, 195415.
- 42 D. Baranov, L. Manna and A. G. Kanaras, *J. Mater. Chem.*, 2011, **21**, 16694–16703.
- 43 Z. H. Tang, C. F. Zeng, Y. D. Lei, B. C. Guo, L. Q. Zhang and D. M. Jia, *J. Mater. Chem.*, 2011, **21**, 17111–17118.
- 44 Z. R. Yue, K. R. Benak, J. W. Wang, C. L. Mangun and J. Economy, *J. Mater. Chem.*, 2005, **15**, 3142–3148.
- 45 Z. P. Zhang and M. Y. Han, *J. Mater. Chem.*, 2003, **13**, 641–643.
- 46 K. J. Lee, W. K. Oh, J. Y. Song, S. J. Kim, J. W. Lee and J. Jang, *Chem. Commun.*, 2010, **46**, 5229–5231.